Multi-rotor Coordinate Transforms for Orthogonal Primary and Redundant Control Modes for Regular Hexacopters and Octocopters

Robert Niemiec
niemir@rpi.edu
Graduate Student
Rensselaer Polytechnic Institute
Troy, NY, United States

Farhan Gandhi
fgandhi@rpi.edu
Redfern Professor of Aerospace Engineering
Rensselaer Polytechnic Institute
Troy, NY, United States

ABSTRACT

This study develops the multi-rotor coordinate transformation, and for hexacopters and octocopters identifies primary and redundant controls in multi-rotor coordinates. For hexacopters, the control modes in multi-rotor coordinates comprise of four primary control modes (the collective, roll, pitch and yaw modes), and two redundant modes (twist and lift-share modes). For octocopters, in addition to the four primary control modes, there are four redundant modes. Two of the redundant modes are twisting modes, the third and fourth are roll-share and pitch-share modes. For both hexacopters and occtocopters, the paper discusses the differences in the control modes between the vertex-first and edge-first orientations. Trim results over the 0-10m/s airspeed range indicate that minimum power flight corresponds to the use of only the primary control modes (with zero redundant controls). The use of certain redundant controls can result in significant changes to the primary controls. The paper also examines the flight dynamic characteristics of hexacopters and octocopters. At moderate forward speed, use of the lift-share redundant control mode was seen to improve the phugoid mode damping of the hexacopter by 10% (at a 1% power penalty cost).

NOTATION

A	Linearized Aircraft Plant Model
$\bar{A}$	Reduced Aircraft Plant Model
A_{11}	Rigid Body Stability Derivatives
A_{12}	Rigid Body - Inflow Stability Derivatives
A_{21}	Inflow - Rigid Body Stability Derivatives
A_{22}	Inflow Stability Derivatives
B	Linearized Control Derivatives
$\bar{B}$	Reduced Control Derivatives
B_1	Rigid Body Control Derivatives
B_2	Inflow Control Derivatives
CCW	Counter-clockwise
CW	Clockwise
$\vec{F}_i$	Linear forces on rotor i – N
m	Maximum inflow harmonic in Peters-He wake model
$\vec{M}_i$	Moments about hub on rotor i – N m
n	Highest radial polynomial in Peters-He model
R	Rotor radius – m
RPM	Revolutions per minute
α_n^m	Longitudinal inflow state
β_n^m	Lateral inflow state
ρ	Air density – $\frac{\text{kg}}{\text{m}^3}$
τ_n^{mc}	Longitudinal inflow forcing parameter
τ_n^{ms}	Lateral inflow forcing parameter
ψ	Blade azimuth – rad
Ψ	Azimuthal location on aircraft – rad
Ω_0	Collective Control – RPM
Ω_d	Yaw Control – RPM
Ω_{ic}	i^{th} harmonic cosine control
Ω_{is}	i^{th} harmonic sine control
Ω_i	Rotational speed of rotor i – $\frac{\text{rad}}{\text{s}}$

Presented at the 42nd Annual European Rotorcraft Forum, Lille, France, September 5–8, 2016.

INTRODUCTION

Recently, there has been tremendous interest in multirotor helicopters for a broad range of applications ranging from defense, border and homeland security, law enforcement, and disaster relief, to commercial applications such as pipeline inspection, crop spraying, land surveys, aerial videography, and package delivery. The simplicity associated with fixed-pitch, variable RPM rotors and distributed electric propulsion has reduced the barrier to entry, and a number of different configurations are available from a number of manufacturers/suppliers. The simplest multirotor configuration is the quadcopter, with each of the four adjacent rotors spinning in opposite directions. Also common are regular hexacopters and octocopters having, respectively, six and eight equally spaced rotors, with adjacent rotors again spinning in opposite directions.

The quadcopter has four independent controls available (the RPM of each of the four rotors). Along with the pitch and roll attitudes, these form a set of six trim variables used to satisfy equilibrium of forces and moments about three axes in steady level flight. Since the number of trim variables is equal to the number of equilibrium equations, the trim solution for a quadcopter is unique. In the literature, quadcopter

controls have been considered in a couple of different ways – either as a vector of *individual rotor controls* (Ω_1, Ω_2, Ω_3, Ω_4), as in (Ref. 1) - (Ref. 4), or as a vector of *multi-rotor controls* about different axes (Ω_0, Ω_R, Ω_P, Ω_Y), as in (Ref. 5) and (Ref. 6), or as the authors have in (Ref. 7) and (Ref. 8). For a quadcopter in the cross-configuration Figs. 1(a)-1(d) show collective control, Ω_0, where all four rotors are sped up to increase thrust, roll control, Ω_R, where the two right rotors are sped up while the two left rotors are slowed down to generate a roll-left moment, pitch control, Ω_P, where the two rear rotors are sped up while the two front rotors are slowed down to generate a nose-down pitch moment, and yaw control, Ω_Y, where the two CW rotors are sped up and the two CCW rotors slowed down to induce a nose-left yaw moment.

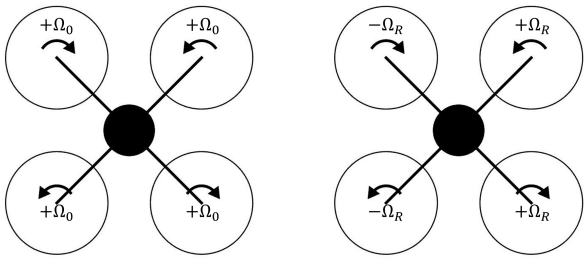

(a) Collective Control (Ω_0) (b) Roll Control (Ω_R)

(c) Pitch Control (Ω_P) (d) Yaw Control (Ω_Y)

Fig. 1. Multi-rotor controls for a quadcopter

A significant advantage of using this set of controls is the decoupling it provides between axes. For example, Ω_O changes the thrust without generating any moment, Ω_R generates roll without pitch or yaw, Ω_P generates a pitching moment without generating a roll or yaw moment, and Ω_Y generates a yaw without pitch or roll. In contrast, changing Ω_1 would generate a net change in thrust, pitch, roll, and yaw moment simultaneously (and the same is true for control inputs Ω_2, Ω_3 and Ω_4).

For hexacopters and octocopters, respectively six and eight independent control inputs are available to control four axes (vertical, pitch, roll, and yaw). With such control redundancy available, this paper focuses first on the presentation of a set of orthogonal controls modes for each configuration in the style of Figs. 1(a)-1(d), and their classification into primary and redundant controls. These controls are then used to trim hexacopter and octocopter helicopters over a range of airspeeds, and the minimum power controls are identified. The flight dynamics modes of these aircraft are also examined and preliminary results on the use of redundant control modes for their improvement are presented.

CONTROL MODES AND THE MULTI-ROTOR COORDINATE TRANSFORM

Quadcopter Control Modes

The RPM of individual rotors of a quadcopter can be expressed as a linear combination of the collective, roll, pitch, and yaw control modes shown in Figs. 1(a)-1(d), as expressed below:

$$\begin{bmatrix}\Omega_1\\ \Omega_2\\ \Omega_3\\ \Omega_4\end{bmatrix} = \begin{bmatrix}1 & 1 & -1 & -1\\ 1 & -1 & -1 & 1\\ 1 & -1 & 1 & -1\\ 1 & 1 & 1 & 1\end{bmatrix}\begin{bmatrix}\Omega_0\\ \Omega_R\\ \Omega_P\\ \Omega_Y\end{bmatrix} \tag{1}$$

In essence, Eq. 1 represents a coordinate transformation from *multi-rotor coordinates* (Ω_0, Ω_R, Ω_P, Ω_Y) to *individual rotor coordinates* (Ω_1, Ω_2, Ω_3, Ω_4), and the column vectors in the matrix represent the collective, roll, pitch, and yaw control modes, respectively. Equation 1 can, in fact, be represented by a mathematical expression such as

$$\Omega_i = \Omega_0 + \Omega_{1s}\sin\Psi_i + \Omega_{1c}\cos\Psi_i + \Omega_d(-1)^i \tag{2}$$

similar to the multi-blade transformation (Ref. 9) used, for example, to convert from individual blade degrees of freedom to rotor collective, longitudinal and lateral cyclic, and differential modes. Using $\Psi = 0^\circ$ at the tail of the aircraft, increasing counterclockwise (so $\Psi_1 = 135^\circ$, $\Psi_2 = 225^\circ$, $\Psi_3 = 315^\circ$, and $\Psi_4 = 45^\circ$ in Fig. 1), Eq. 2 expands to:

$$\begin{bmatrix}\Omega_1\\ \Omega_2\\ \Omega_3\\ \Omega_4\end{bmatrix} = \begin{bmatrix}1 & 1/\sqrt{2} & -1/\sqrt{2} & -1\\ 1 & -1/\sqrt{2} & -1/\sqrt{2} & 1\\ 1 & -1/\sqrt{2} & 1/\sqrt{2} & -1\\ 1 & 1/\sqrt{2} & 1/\sqrt{2} & 1\end{bmatrix}\begin{bmatrix}\Omega_0\\ \Omega_{1s}\\ \Omega_{1c}\\ \Omega_d\end{bmatrix} \tag{3}$$

The columns in the matrix in Eq. 3 are simply mode shapes, and it is easy to see that the second column introduces a roll moment on the aircraft and that the third introduces a pitch moment. Since the columns are mode shapes, a $1/\sqrt{2}$ scaling factor can be removed from columns 2 and 3. With these changes, Eq. 3 can be written as:

$$\begin{bmatrix}\Omega_1\\ \Omega_2\\ \Omega_3\\ \Omega_4\end{bmatrix} = \begin{bmatrix}1 & 1 & -1 & -1\\ 1 & -1 & -1 & 1\\ 1 & -1 & 1 & -1\\ 1 & 1 & 1 & 1\end{bmatrix}\begin{bmatrix}\Omega_0\\ \Omega_{1s}\\ \Omega_{1c}\\ \Omega_d\end{bmatrix} \tag{4}$$

which is identical to Eq. 1, with Ω_0 still representing collective control, and Ω_{1s}, Ω_{1c}, and Ω_d corresponding to roll, pitch, and yaw control, respectively. The multi-rotor control modes (columns of equation 4) are orthogonal, and this is ensured by the nature of Eq. 2.

Primary and Redundant Multi-Rotor Control Modes for a Hexacopter

A regular hexacopter with equally-spaced rotors typically assumes one of two configurations in operation: vertex-first or edge-first, as shown in Fig. 2. With six individual rotor controls for a hexacopter (Ω_1, Ω_2, Ω_3, ..., Ω_6), the multirotor coordinate transformation can be written as:

$$\begin{aligned}\Omega_i = \Omega_0 &+ \Omega_{1s}\sin(\Psi_i) \;+\Omega_{1c}\cos(\Psi_i) + \Omega_d(-1)^i \\ &+\Omega_{2s}\sin(2\Psi_i) + \Omega_{2c}\cos(2\Psi_i)\end{aligned} \tag{5}$$

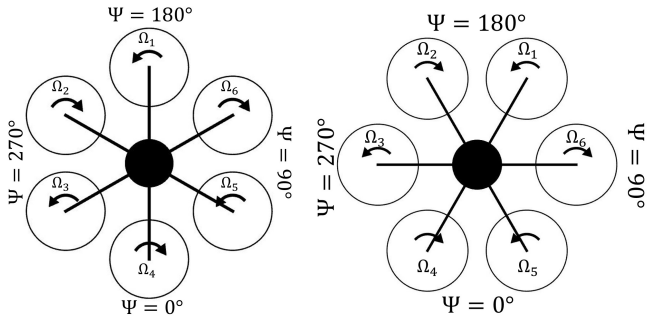

(a) Vertex First (b) Edge First

Fig. 2. Hexacopter orientations

Second harmonic terms are introduced on the right-hand side as the number of multi-rotor controls must be the same as the number of individual rotor controls (which is equal to the number of rotors). The multi-rotor controls for the hexacopter are then Ω_0, Ω_{1s}, Ω_{1c}, Ω_d, Ω_{2s}, and Ω_{2c}, and the terms of the series in Eq. 5, by their very nature, ensures orthogonality of the multi-rotor controls modes for the hexacopter. For the vertex-first case (Fig. 2(a)), and $\Psi = 0$ at the tail of the aircraft (so $\Psi_1 = 180°$, $\Psi_2 = 240°$, $\Psi_3 = 300°$, $\Psi_4 = 0°$, $\Psi_5 = 60°$, $\Psi_6 = 120°$), Eq. 5 expands to:

$$\begin{bmatrix}\Omega_1\\ \Omega_2\\ \Omega_3\\ \Omega_4\\ \Omega_5\\ \Omega_6\end{bmatrix} = \begin{bmatrix}1 & 0 & -2 & -1 & 0 & 2\\ 1 & -1 & -1 & 1 & 1 & -1\\ 1 & -1 & 1 & -1 & -1 & -1\\ 1 & 0 & 2 & 1 & 0 & 2\\ 1 & 1 & 1 & -1 & 1 & -1\\ 1 & 1 & -1 & 1 & -1 & -1\end{bmatrix}\begin{bmatrix}\Omega_0\\ \Omega_{1s}\\ \Omega_{1c}\\ \Omega_d\\ \Omega_{2s}\\ \Omega_{2c}\end{bmatrix} \tag{6}$$

As with the quadcopter, Ω_0 represents collective control, and the collective mode (first column of matrix in Eq. 6), which generates thrust, speeds all rotors by the same amount (Fig. 3(a)). Ω_{1s} represents the roll control in multi-rotor coordinates, and the roll control mode (second matrix column in Eq. 6) slows the two left rotors and speeds up the two right rotors, while the front and rear rotor are unused (Fig. 3(b)). Ω_{1c} represents pitch control in multi-rotor coordinates, and the pitch control mode (third matrix column in Eq. 6) slows the three front rotors while speeding up the three aft rotors (Fig. 3(c)). It should be noted that the RPM change for the front-most and rear-most rotors (rotors 1 and 4 in Fig. 3(c)) is twice that for the rotors closer to the lateral axis (2, 3, 5, and 6). Ω_d represents yaw control, and, as with the quadcopter, the yaw control mode speeds up clockwise rotors while slowing the counterclockwise rotors, for a nose-left yaw (Fig. 3(d)). These four modes are the primary controls for the hexacopter in the vertex-first orientation.

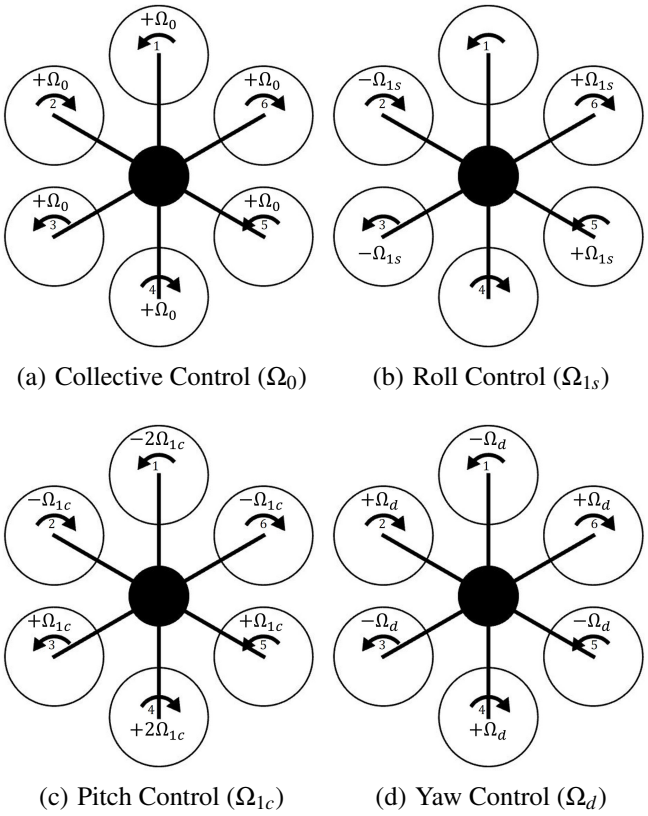

(a) Collective Control (Ω_0) (b) Roll Control (Ω_{1s})

(c) Pitch Control (Ω_{1c}) (d) Yaw Control (Ω_d)

Fig. 3. Primary multi-rotor controls for a hexacopter in vertex-first orientation

The modes corresponding to the fifth and sixth columns in Eq. 6 are shown in Fig. 4. The Ω_{2s} mode (Fig. 4(a)) slows the northeast and southwest rotors (6 and 3) while speeding up the southeast and northwest rotors (5 and 2), resulting in a *twisting action about the lateral and longitudinal axes*. The Ω_{2c} mode (Fig. 4(b)), speeds up the front- and aft-most rotors while slowing the four rotors offset from the longitudinal axis (2, 3, 5, and 6). With the increase in RPM for rotors 1 and 4 being twice the reduction in rotors 2, 3, 5, and 6, this mode changes lift share between the longitudinally offset and vertex rotors (without any significant changes in net thrust, pitch, roll, or yaw moment). The twist and lift share modes are the two redundant control modes, and are orthogonal to each other as well as to the primary control modes described in the preceding paragraph.

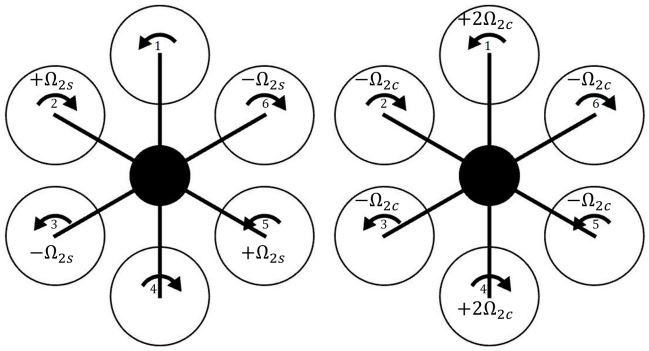

(a) Twist (Ω_{2s}) (b) Lift Share (Ω_{2c})

Fig. 4. Redundant multi-rotor controls for a hexacopter in vertex-first orientation

For a hexacopter operating edge-first, as in Fig. 2(b), setting $\Psi_1 = 150°$, $\Psi_2 = 210°$, $\Psi_3 = 270°$, $\Psi_4 = 330°$, $\Psi_5 = 30°$, and $\Psi_6 = 90°$, Eq. 5 expands to:

$$\begin{bmatrix} \Omega_1 \\ \Omega_2 \\ \Omega_3 \\ \Omega_4 \\ \Omega_5 \\ \Omega_6 \end{bmatrix} = \begin{bmatrix} 1 & 1 & -1 & -1 & -1 & 1 \\ 1 & -1 & -1 & 1 & 1 & 1 \\ 1 & -2 & 0 & -1 & 0 & -2 \\ 1 & -1 & 1 & 1 & -1 & 1 \\ 1 & 1 & 1 & -1 & 1 & 1 \\ 1 & 2 & 0 & 1 & 0 & -2 \end{bmatrix} \begin{bmatrix} \Omega_0 \\ \Omega_{1s} \\ \Omega_{1c} \\ \Omega_d \\ \Omega_{2s} \\ \Omega_{2c} \end{bmatrix} \tag{7}$$

The collective mode, associated with the control Ω_0 (Fig. 5(a)), speeds up all rotors equally to change net thrust, just like the vertex-first case. The roll mode, associated with Ω_{1s}, slows the three left rotors and speeds up the three right rotors (Fig. 5(b)), The RPM change for the vertex rotors is twice that of the rotors closer to the longitudinal axis. The pitch control mode, associated with Ω_{1c}, slows the two front rotors and speeds the two aft rotors, while the vertex rotors are unused (Fig. 5(c)). The yaw mode, associated with the control Ω_d, slows the counterclockwise rotors and speeds up the clockwise rotors to generate a nose-left moment (Fig. 5(d)), as in the vertex-first case. These four modes are the primary control modes for the hexacopter in the edge-first orientation.

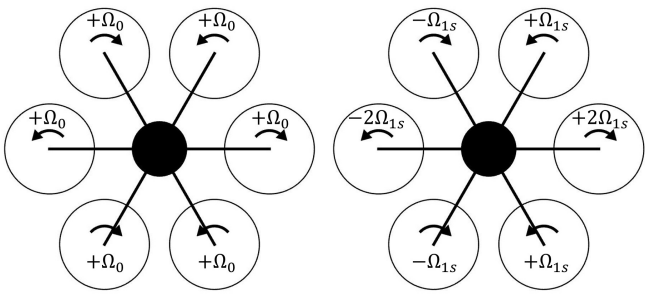

(a) Collective Control (Ω_0 (b) Roll Control (Ω_{1s})

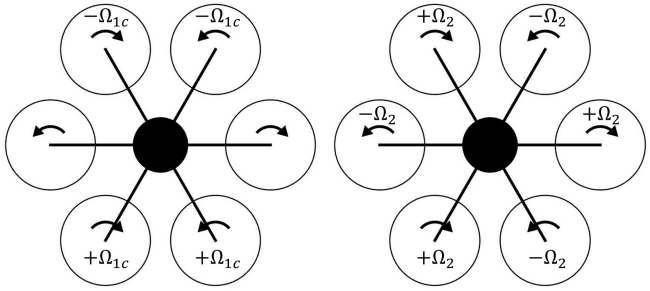

(c) Pitch Control (Ω_{1c}) (d) Yaw Control (Ω_d)

Fig. 5. Primary multi-rotor controls for a hexacopter in edge-first orientation

The redundant control modes for the edge-first case are shown in Fig. 6. As was the case for the vertex-first orientation, the Ω_{2s} mode (Fig. 6(a)) also generates a *twisting action about the lateral and longitudinal axes*, without any other net moments. The Ω_{2c} mode (Fig. 6(b)) slows down the rotors along the lateral axis while speeding up the front and aft rotors (1, 2, 4, and 5), and this control changes the *lift share* between the rotors (without generating any significant net lift, roll, pitch, or yaw moment).

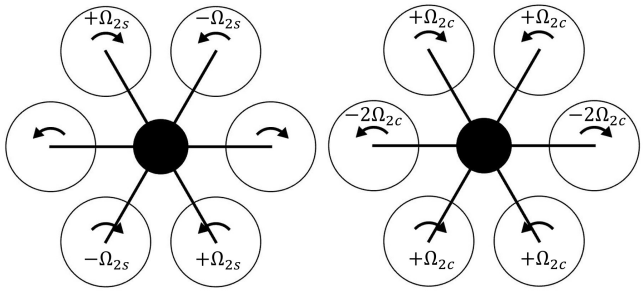

(a) Twist (Ω_{2s}) (b) Lift Share (Ω_{2c})

Fig. 6. Redundant multi-rotor controls for hexacopter in edge first orientation

From a comparison of the vertex-first and edge-first orientations, the following observations can be drawn for the primary control modes of the hexacopter: the collective and yaw control modes are the same; four rotors are used for roll in the vertex-first case, while four are used for pitch in the edge-first case; six rotors are used for pitch in the vertex-first case, and for roll in the edge-first case. In these cases, the change in the vertex rotors' RPM (1 and 4 for the vertex-first, 3 and 6 for edge-first) is twice the change experienced by the other four rotors. An examination of the redundant modes reveals that the vertex-first as well as the edge-first orientations have a twist mode and both orientations include a lift share mode that distributes lift between the vertex rotors and those closer to the lateral and longitudinal axes.

Primary and Redundant Multi-Rotor Control Modes for an Octocopter

Like the hexacopter, a regular octocopter with equally spaced rotors can operate in vertex-first or edge-first orientations, as shown in Fig. 7. With eight individual rotor controls for an octocopter (Ω_1, Ω_2, Ω_3, …, Ω_8), the multi-rotor coordinate transformation can be written as:

$$\begin{aligned}\Omega_i = \Omega_0 &+ \Omega_{1s}\sin(\Psi_i) + \Omega_{1c}\cos(\Psi_i) + \Omega_2(-1)^i \\ &+ \Omega_{2s}\sin(2\Psi_i) + \Omega_{2c}\cos(2\Psi_i) \\ &+ \Omega_{3s}\sin(3\Psi_i) + \Omega_{3c}\cos(3\Psi_i)\end{aligned} \tag{8}$$

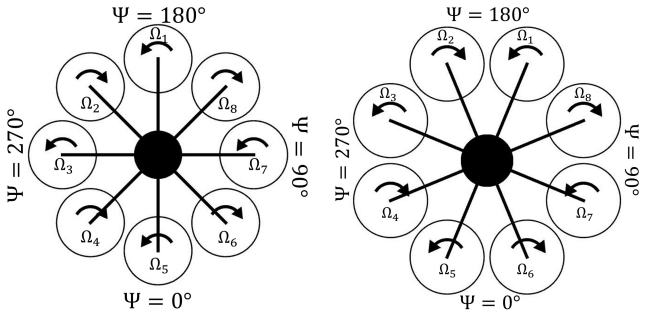

(a) Vertex First (b) Edge First

Fig. 7. Octocopter Orientations

Additional third harmonic terms introduced on the right-hand side result in eight multi-rotor controls equal to the number of rotors and individual controls. For the vertex-first case (Fig. 7(a)) and $\Psi = 0$ pointing towards the tail of the aircraft, $\Psi_1 = 180°$, $\Psi_2 = 225°$, $\Psi_3 = 270°$, $\Psi_4 = 315°$, $\Psi_5 = 0°$, $\Psi_6 = 45°$, $\Psi_7 = 90°$, and $\Psi_8 = 135°$, and Eq. 8 expands to:

$$\begin{bmatrix}\Omega_1\\ \Omega_2\\ \Omega_3\\ \Omega_4\\ \Omega_5\\ \Omega_6\\ \Omega_7\\ \Omega_8\end{bmatrix} = \begin{bmatrix}1 & 0 & -k & -1 & 0 & 1 & 0 & -k\\ 1 & -1 & -1 & 1 & 1 & 0 & -1 & 1\\ 1 & -k & 0 & -1 & 0 & -1 & k & 0\\ 1 & -1 & 1 & 1 & -1 & 0 & -1 & -1\\ 1 & 0 & k & -1 & 0 & 1 & 0 & k\\ 1 & 1 & 1 & 1 & 1 & 0 & 1 & -1\\ 1 & k & 0 & -1 & 0 & -1 & -k & 0\\ 1 & 1 & -1 & 1 & -1 & 0 & 1 & 1\end{bmatrix} \begin{bmatrix}\Omega_0\\ \Omega_{1s}\\ \Omega_{1c}\\ \Omega_d\\ \Omega_{2s}\\ \Omega_{2c}\\ \Omega_{3s}\\ \Omega_{3c}\end{bmatrix} \tag{9}$$

where $k = \sqrt{2}$. As with the quadcopter and hexacopter, Ω_0 represents collective control, and the collective mode (first column in the matrix in Eq. 9) generates thrust by changing the speed of all rotors equally (Fig. 8(a)). Ω_{1s} represents roll control, and the roll control mode (second column in matrix) slows the three left rotors and speeds the three right rotors, while the front and aft rotors are not used (Fig. 8(b)). The change in RPM for the left-most and right-most rotors is greater than that in the immediately adjacent rotors by a factor of $\sqrt{2}$. Ω_{1c} represents the pitch control in multi-rotor coordinates, and the pitch control mode (third column in the matrix) slows the front three rotors, and speeds up the rear three rotors. The change in RPM of the front-most and aft-most rotors is a factor of $\sqrt{2}$ times greater than their adjacent rotors (Fig. 8(c)). A comparison of Figs. 8(b) and 8(c) shows that the pitch control mode is, in fact, the roll control mode rotated by 90°, similar to the quadcopter. Ω_d represents yaw control in multi-rotor coordinates, and as with the quadcopter and hexacopter, the yaw control mode (the fourth column in the matrix), slows the counterclockwise rotors and speeds up the clockwise rotors (Fig. 8(d)). These four modes are the primary orthogonal modes for the octocopter in the vertex-first configuration.

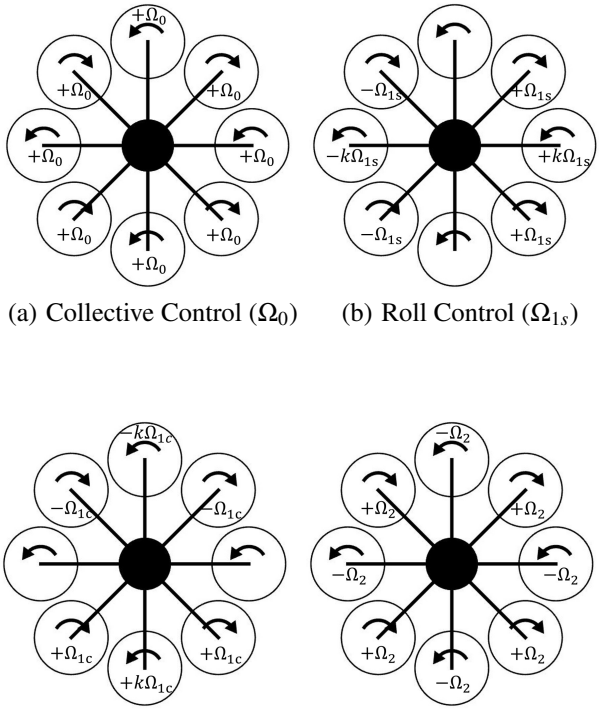

(a) Collective Control (Ω_0) (b) Roll Control (Ω_{1s})

(c) Pitch Control (Ω_{1c}) (d) Yaw Control Ω_d

Fig. 8. Primary multi-rotor controls for octocopter in vertex-first orientation

The modes corresponding to the fifth through eighth columns of the matrix in Eq. 9 are shown in Fig. 9. The Ω_{2s} mode (column five and shown in Fig. 9(a)) is a *clockwise rotor lift-share mode* with lift transferring from the 135°-−315° axis toward the 45°−225° axis. This mode does not use the counterclockwise rotors whatsoever, and does not generate any pitch, roll, or yaw moments. This mode can also be interpreted as a twisting mode about the 0°−180° and the 90°−270° axes. Similarly, the Ω_{2c} mode (column six in the matrix and shown in Fig. 9(b)), is a *counterclockwise rotor lift-share mode*, with lift transferring from the 90°−270° axis. this mode does not use the clockwise rotors, and again does not generate any net moments. This mode can also be interpreted as a twist about the 45°−225° and 135°−315° axes.

The Ω_{3s} mode (column seven, Fig. 9(c)) is a *roll-share mode*, with the left- and right-most rotors producing a roll mo-

ment opposite in sense to that produced by the combinations of rotors 2, 4, 6, and 8 (the front and aft rotors are not used). The RPM changes to the left- and right-most rotors is a factor $\sqrt{2}$ greater than the changes in the other four rotors, such that the net rolling moment produced is zero. Similarly, the Ω_{3c} mode (column eight, Fig. 9(d)), is a *pitch-share mode*, with the front- and rear-most rotors (along the longitudinal axis) applying a pitching moment opposite in sense to the pitching moment applied by the combination of the four rotors (2, 4, 6, and 8) closer to the lateral axis, while the left- and right-most rotors are not used. Similar to the roll-share (Ω_{3s}), the RPM changes to the front- and rear-most rotors is a factor $\sqrt{2}$ greater than the change in the other four, in order to equilibrate the pitching moment.

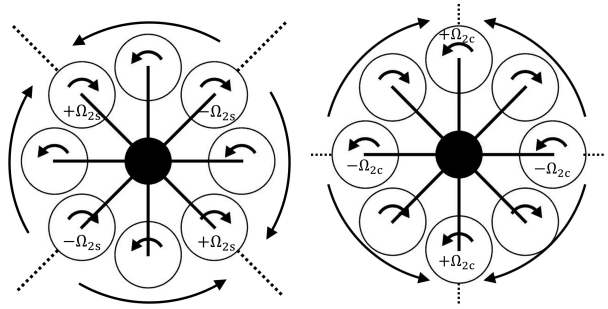

(a) CW Lift Sharing (b) CCW Lift Sharing

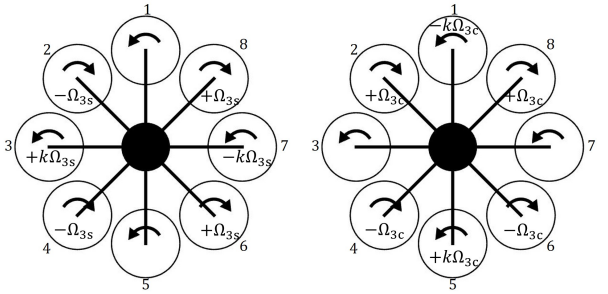

(c) Roll Sharing (d) Pitch Sharing

Fig. 9. Redundant multi-rotor controls for octocopter in vertex-first orientation

For an octocopter operating edge-first (Fig. 7(b)), $\Psi_1 = 157.5°$, $\Psi_2 = 202.5°$, $\Psi_3 = 247.5°$, $\Psi_4 = 292.5°$, $\Psi_5 = 337.5°$, $\Psi_6 = 22.5°$, $\Psi_7 = 67.5°$, and $\Psi_8 = 112.5°$, and Eq. 8 expands to:

$$\begin{bmatrix}\Omega_1\\ \Omega_2\\ \Omega_3\\ \Omega_4\\ \Omega_5\\ \Omega_6\\ \Omega_7\\ \Omega_8\end{bmatrix} = \begin{bmatrix}1 & 1 & -k & -1 & -1 & 1 & k & -1\\ 1 & -1 & -k & 1 & 1 & 1 & -k & -1\\ 1 & -k & -1 & -1 & 1 & -1 & 1 & k\\ 1 & -k & 1 & 1 & -1 & -1 & 1 & -k\\ 1 & -1 & k & -1 & -1 & 1 & -k & 1\\ 1 & 1 & k & 1 & 1 & 1 & k & 1\\ 1 & k & 1 & -1 & 1 & -1 & -1 & -k\\ 1 & k & -1 & 1 & -1 & -1 & -1 & k\end{bmatrix} \begin{bmatrix}\Omega_0\\ \Omega_{1s}\\ \Omega_{1c}\\ \Omega_d\\ \Omega_{2s}\\ \Omega_{2c}\\ \Omega_{3s}\\ \Omega_{3c}\end{bmatrix} \tag{10}$$

where $k = 1+\sqrt{2}$. The collective mode, associated with the control Ω_0, speeds up all the rotors equally as shown in Fig. 10(a) to generate a net thrust, just like the vertex-first case (Fig. 8(a)). The roll mode, associated with the control Ω_{1s}, slows down the four rotors on one side of the longitudinal axis while speeding up the four rotors on the other side (Fig. 10(b)). On any given side, the change in RPM of the two rotors farthest from the longitudinal axis is a factor $(1+\sqrt{2})$ greater than the RPM change of the two closer rotors. The pitch mode, associated with the control Ω_{1c}, slows down the four rotors on one side of the lateral axis while speeding up the four rotors on the other side (Fig. 10(c)). Similar to the roll mode, the change in RPM of the two rotors farthest from the lateral axis is a factor $(1+\sqrt{2})$ greater than the RPM change corresponding to the two closer rotors. A comparison of Figs. 10(b) and 10(c) shows that the pitch mode is, in fact, the roll mode rotated by 90°, as was the case for the vertex-first orientation. The yaw mode, associated with the control Ω_d, slows the counter-clockwise rotors while speeding up the clockwise rotors (Fig. 10(d)), just like the vertex-first case (Fig. 8(d)). These four modes represent the primary control modes in multi-rotor coordinates for the edge-first octocopter case.

The modes corresponding to the fifth through eighth columns of the matrix in Eq. 10 are shown in Fig. 11. As in the vertex-first case, the Ω_{2s} mode (Fig. 11(a)) transfers lift from the $135° - 315°$ axis toward the $45° - 225°$ axis. This mode can also be interpreted as having a twisting action about the longitudinal and lateral axes. Similarly, the Ω_{2c} mode (Fig. 11(b)) transfers lift from the $90° - 270°$ axis toward the $0° - 180°$ axis and can be interpreted as a twisting action about the $45° - 225°$ and $135° - 315°$ axes.

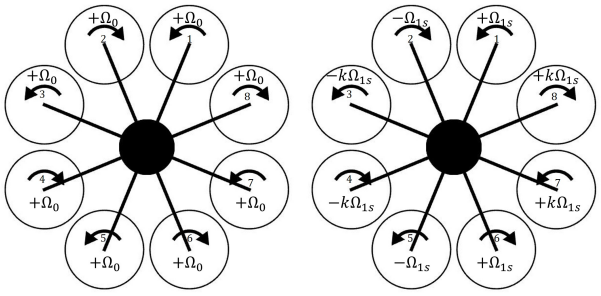

(a) Collective Control (Ω_0) (b) Roll Control (Ω_{1s})

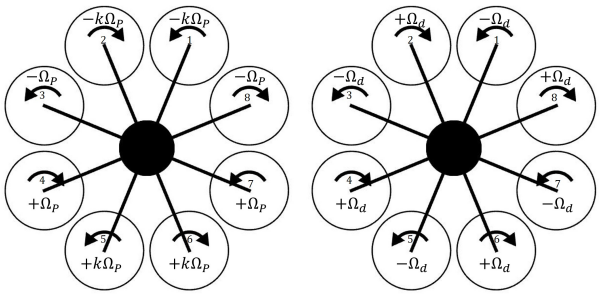

(c) Pitch Control (Ω_{1c}) (d) Yaw Control (Ω_d)

Fig. 10. Primary multi-rotor controls for the octocopter in edge-first orientation

The Ω_{3s} mode (Fig. 11(c)) is a *roll-share mode*, with the two left-most and two right-most rotors applying a roll moment that is opposite in sense to that produced by the rotors closer to the longitudinal axis. The RPM changes to the rotors closest to the roll axis is a factor k greater than the changes to the left- and right-most rotors, such that the net roll moment produced is zero. Similarly the Ω_{3c} mode (Fig. 11(d) is a *pitch-share mode*, with the two front-most and two rear-most rotors applying a pitching moment opposite in sense to that produced by the four rotors closest to the lateral axis. The RPM changes to these four rotors is a factor k greater than that applied to the front- and rear-most rotors, so that the net pitching moment is zero (as are the lift, roll moment, and yaw moment produced).

A comparison of the vertex-first and edge-first octocopter orientations shows that of the primary control modes, while the collective and yaw control modes are similar, the roll and pitch control modes use all 8 rotors for the edge-first case, but only 6 rotors for the vertex-first case since the latter has two rotors on the longitudinal axis (that provide no roll authority) and two on the lateral axis (that provide no pitch authority). The Ω_{2s}, Ω_{2c} redundant modes apply a twisting action to both the vertex-first and edge-first orientations. For the vertex-first orientation, the Ω_{2s} mode can also be identified as lift-share mode between clockwise spinning rotors, and the Ω_{2c} mode can similarly be identified as a lift-share mode between the counterclockwise rotors. For both octocopter orientations, the Ω_{3s} and Ω_{3c} redundant modes are roll-share and pitch-share modes, respectively, but as with the primary roll and pitch control modes, the vertex-first orientation uses only 6 rotors as opposed to the edge-first orientation which uses all 8.

MODELING

To assess the performance of the multirotor helicopters in various flight conditions, a nonlinear dynamic analysis was constructed. It determines the accelerations of the aircraft using a summation of forces and moments about a point in the geometric center of the aircraft, in the same plane as the rotors, using the aircraft states and control inputs as arguments. These forces include gravity, which acts at the center of gravity, assumed to be located directly beneath the reference point, fuselage drag, and rotor forces.

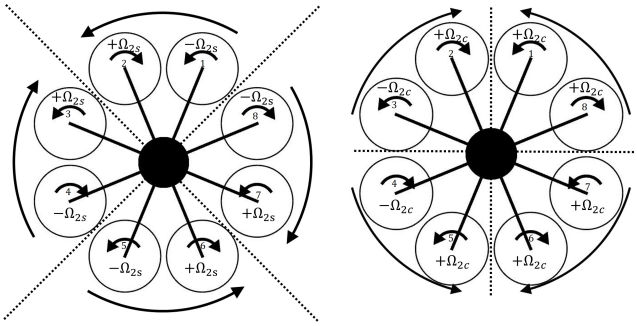

(a) Ω_{2s} Mode (b) Ω_{2c} Mode

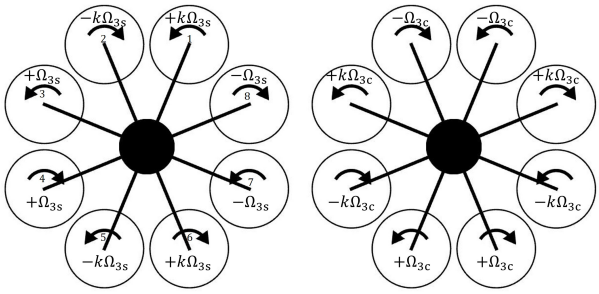

(c) Roll Share (d) Pitch Share

Fig. 11. Redundant multi-rotor controls for the octocopter in edge-first orientation

Rotor forces are calculated individually using Blade Element Theory. At each blade element of width dr, aerodynamic forces are evaluated from the resultant velocity (driven by freestream velocity, rotor rotation, and inflow velocity) and the aerodynamic properties of the airfoil as it sweeps through $d\psi$. The airfoils used were a pure Clark Y at the root, and a pure NACA4412 at the tip, with airfoil properties linearly interpolated along the span. Elemental forces are integrated along the span of the rotor blade, and then averaged about a rotor revolution to obtain the average rotor forces and moments about the hub (equation 11). This results in a 6-element force vector per rotor, with three linear forces and three moments.

$$\begin{aligned} \vec{F}_i &= \frac{1}{2\pi}\int_0^{2\pi}\int_0^R \vec{F}(r,\psi)drd\psi \\ \vec{M}_i &= \frac{1}{2\pi}\int_0^{2\pi}\int_0^R (\vec{F}(r,\psi)\times\vec{r})drd\psi \end{aligned} \tag{11}$$

where $\vec{F}$ is the force at the blade element, and $\vec{r}$ is a vector from the hub to the blade element.

The rotor and aircraft geometries are given in Table 1. The rotors are sized such that the two aircraft have the same total

disk area as the AeroQuad Cyclone ARF kit (Fig. 12), which uses four 12 inch diameter rotors. The blades are assumed to be linearly tapered and linearly twisted, with root and tip solidities and pitch measured from the 12x5.5 propellers pictured in Fig. 12.

Table 1. Aircraft Geometry

Property	Hexacopter	Octocopter
Rotor Radius (m)	0.1245	0.1078
Root Solidity	0.13	0.13
Tip Solidity	0.0514	0.0514
Root Pitch	21.5°	21.5 °
Blade Twist	-10.4°	-10.4°
Boom Length (m)	0.3048	0.3048
GTOW (kg)	2	2

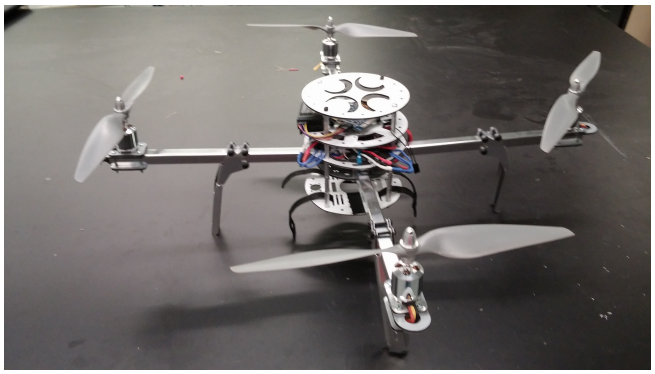

Fig. 12. Aeroquad Cyclone ARF kit

The inflow model used is the 3x4 Peters-He Dynamic Wake model, with 10 inflow states per rotor. This model uses a first-order differential equation to determine the derivatives of these inflow states, forced by the aerodynamic thrust distribution. The governing equation of the inflow distribution is given by equation 12

$$\begin{aligned} \Omega K \dot{\alpha}_n^m + V[L^c]^{(-1)} \alpha_n^m &= \frac{1}{2}\tau_n^{mc} \\ \Omega K \dot{\beta}_n^m + V[L^s]^{(-1)} \beta_n^m &= \frac{1}{2}\tau_n^{ms} \end{aligned} \tag{12}$$

where

$$\begin{aligned} \tau_n^{0c} &= \frac{N_{blades}}{4\pi^2}\int_0^{2\pi}\int_0^R \frac{L}{\rho\Omega^2 R^4}\phi_n^0(r/R)drd\psi \\ \tau_n^{mc} &= \frac{N_{blades}}{2\pi^2}\int_0^{2\pi}\left[\int_0^R \frac{L}{\rho\Omega^2 R^4}\phi_n^m(r/R)dr\right]\cos(m\psi)d\psi \\ \tau_n^{ms} &= \frac{N_{blades}}{2\pi^2}\int_0^{2\pi}\left[\int_0^R \frac{L}{\rho\Omega^2 R^4}\phi_n^m(r/R)dr\right]\sin(m\psi)d\psi \end{aligned}$$

where ϕ_n^m is an $(n-1)^{\text{th}}$ order polynomial. As with the rotor forces and moments, the inflow forcing is averaged over a rotor revolution.

In order to perform a trim analysis on the hexacopter and octocopter, the redundant controls are fixed initially set to zero (subsequently varied parametrically), and the 4 primary controls are solved, along with the pitch and roll attitudes, such that the calculated accelerations are equal to zero. Additionally, the Peters-He dynamic wake equations are solved such that the inflow states are in a steady-state condition.

To explore the effects of the redundant controls on the trim controls of the hexacopter helicopter, each was varied parametrically between -1000 RPM and 1000 RPM, one at a time, to generate a family of curves for each of the primary controls. The first thing to note is that because the controls are linearly independent (a necessary condition for orthogonality), varying the redundant controls is guaranteed to change the trim solution. However, the required pitch and roll attitudes are unaffected by the redundant controls, since the thrust still must be vectored in the same way. Thus, the only differences are to be found in the values of the primary controls.

To analyze the flight dynamics of the hexacopter and octocopter, the nonlinear model is linearized numerically about a trim solution. The linearized model takes the form of the matrix equation 13.

$$\dot{x} = Ax + Bu \tag{13}$$

where

$$\vec{x} = \begin{bmatrix} x & y & z & \phi & \theta & \psi & u & v & w & p & q & r & \vec{\lambda} \end{bmatrix}^T$$
$$\vec{u} = \begin{bmatrix} \Delta\Omega_0 & \Delta\Omega_P & \Delta\Omega_R & \Delta\Omega_Y & \Delta(\text{Redundant Controls}) \end{bmatrix}^T$$

where $\vec{\lambda}$ represenst the inflow states.

Where the entries of A represent the stability derivatives, and the entries of B represent the control derivatives. To simplify analysis, the model is partitioned into two parts: one associated with the rigid body states, and another with the inflow states. After partitioning equation 13, we obtain equation 14.

$$\begin{aligned} \dot{x_1} &= A_{11}x_1 + A_{12}x_2 + B_1 u \\ \dot{x_2} &= A_{21}x_1 + A_{22}x_2 + B_2 u \end{aligned} \tag{14}$$

The inflow states converge extremely quickly, so the technique of static condensation is applied, setting $\dot{x_2} = 0$. Solving the inflow equation for x_2 and substituting into the aircraft model we obtain equation 15

$$\begin{aligned} \dot{x_1} &= (A_{11} - A_{12}A_{22}^{-1}A_{21})x_1 + (B_1 - A_1 2A_{22}^{-1}B_2)u \\ &= \bar{A}x_1 + \bar{B}u \end{aligned} \tag{15}$$

To observe the dynamic modes of the aircraft, u is set to zero, and then equation 15 becomes 16. The eigenvectors of $\bar{A}$ are the rigid body dynamic modes of the aircraft, and the corresponding eigenvalues indicate the stability and frequency of the modes.

$$\dot{x_1} = \bar{A}x_1 \tag{16}$$

TRIM RESULTS

Hexacopter Trim

Trim results over a 0-10 m/s speed range for the vertex-first hexacopter with each of the redundant controls set to zero are given in Fig. 13. In order to maintain altitude and speed, each of the rotors needs to produce a baseline thrust, thus requiring collective control (Ω_0, Fig. 13(a)). As forward speed increases, Ω_0 drops, followed by an increase at higher speed. The drop is due to an increased efficiency in the rotors at moderate forward speeds, while the increase can be attributed to the increase in aircraft drag as speed grows. In order to fly forward, the hexacopter must vector its thrust forward. Absent cyclic inputs, the only way for the aircraft to do so is to pitch nose-down. As the speed increases, the thrust must be vectored increasingly forward, thus requiring a greater nose-down attitude (Fig. 13(c)). To maintin this nose-down attitude, pitch control (Ω_{1c}) must be applied. Positive Ω_{1c} produces a nose-down moment, and increases monotonically with speed (Fig. 13(b)). These controls do not produce any lateral forces or moments, so the roll control, yaw control, and roll attitude are all predicted to be zero.

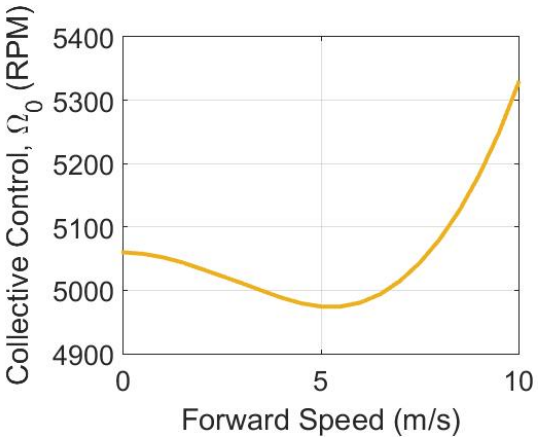

(a) Collective Control

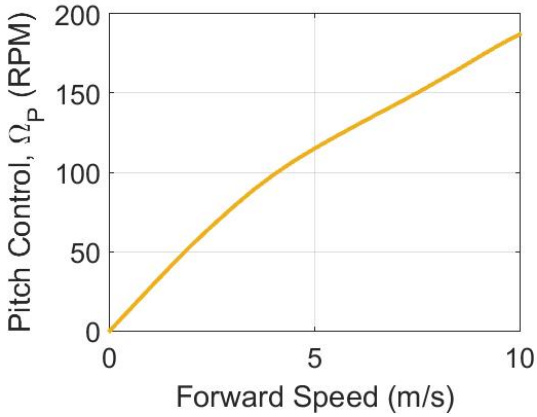

(b) Pitch Control

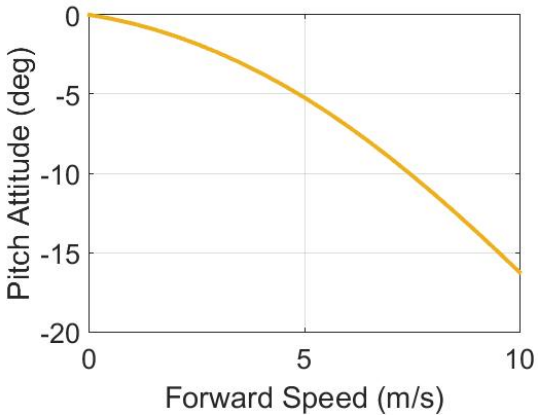

(c) Pitch Attitude

Fig. 13. Hexacopter (vertex-first) trim versus forward flight speed with zero redundant controls

Variation of Redundant Controls on Hexacopter

When only Ω_{2s} is varied, the resulting trim solutions can be found in Fig. 14. As Ω_{2s} is varied from 0, the required collective control input Ω_0 is reduced slightly (Fig. 14(a)). This is because thrust behaves quadratically with RPM, so any control input will produce a net thrust on the aircraft. Increase or decrease in Ω_{2s} results in the same change in collective control.

In the hover condition, roll control (Ω_{1s}, Fig. 14(b)) is not affected by Ω_{2s}, indicating that Ω_{2s} is roll-neutral in hover. However, in forward flight, Ω_{2s} does produce a small rolling moment, which requires compensation by the primary roll control input. Pitch control (Ω_{1c}) is unaffected by Ω_{2s}, indicating that at all forward speeds, Ω_{2s} is pitch-neutral. Yaw control (Ω_d, Fig. 14(c)) is affected in a similar manner as Ω_0, with positive or negative Ω_{2s} producing a yawing moment in the same direction.

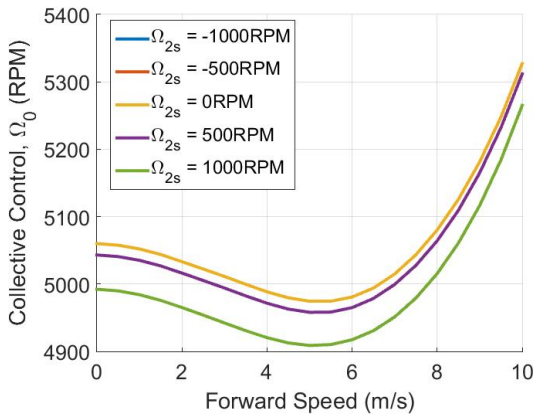

(a) Collective Control

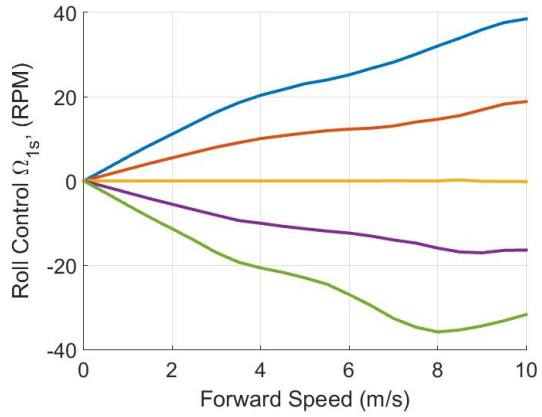

(b) Lateral Control

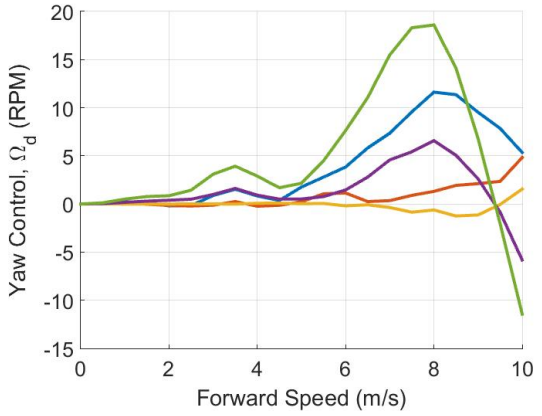

(c) Yaw Control

Fig. 14. Trim Solutions when Ω_{2s} is varied

Next, Ω_{2c} alone is parametrically varied. The resulting trim solutions are presented in Fig. 15. As in the case of Ω_{2s}, Ω_{2c} causes in decrease in Ω_0 (Fig. 15(a)). In hover, Ω_{2c} does not affect any of the other trim controls. In forward flight, increasing Ω_{2c} causes Ω_{1s} to become more negative and Ω_d to become more positive.

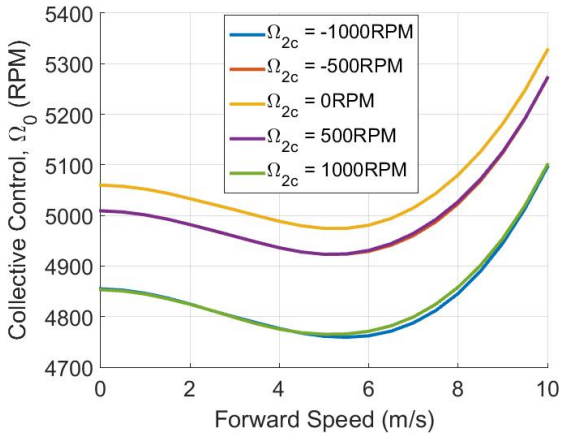

(a) Collective Control

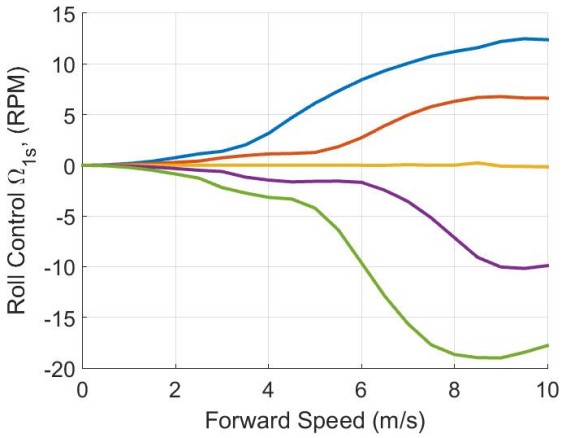

(b) Lateral Control

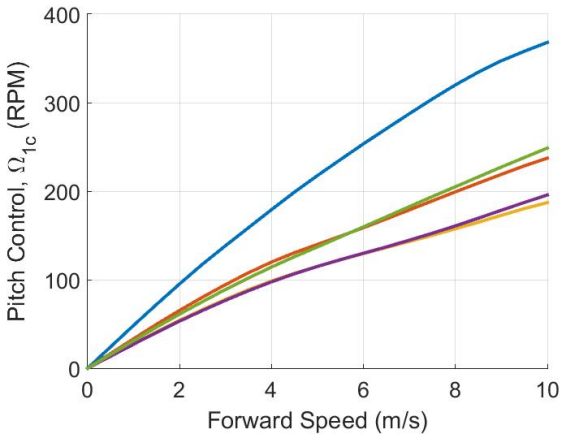

(c) Pitch Control

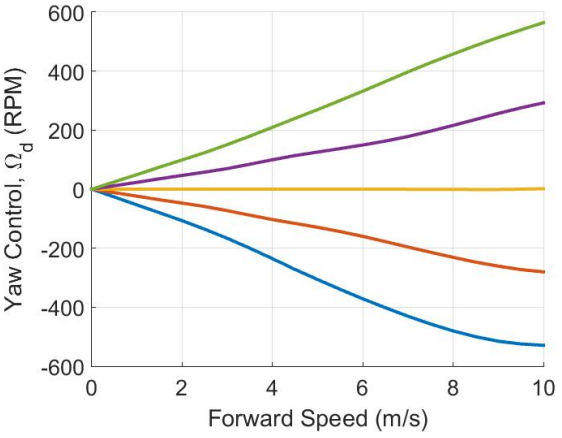

(d) Yaw Control

Fig. 15. Trim Solutions as Ω_{2c} is varied

When Ω_{2c} (plotted in Fig. 15(c)) is negative, lift is shifted from the front and aft rotors (numbered 1 and 4 in Fig. 2) to the left and right rotors (numbered 2, 3, 5, and 6 in Fig. 2).

Rotors 1 and 4 are more effective at producing a pitching moment, since they are farther from the pitch axis, and reducing their lift thus reduces the efficiency of Ω_{1c} in producing moment as shown in (Ref. 8). Therefore, one needs more than the baseline Ω_{1c} to maintain a nose-down attitude. Bringing Ω_{2c} closer to zero balances the lift and makes Ω_{1c} more effective. When Ω_{2c} is zero, Ω_{1c} is at a minimum. Increasing Ω_{2c} above zero leads to an increase in the required pitch control, since the efficiency of the other four rotors in producing pitching moment is reduced, though the penalty is no so great as it is for negative Ω_{2c}.

Finally, Fig. 16 shows the power requirements as a function of the two redundant controls at hover, and 5 m/s and 10 m/s forward flight conditions. For each of these conditions, the minimum power is found at $\Omega_{2s} = \Omega_{2c} = 0$.

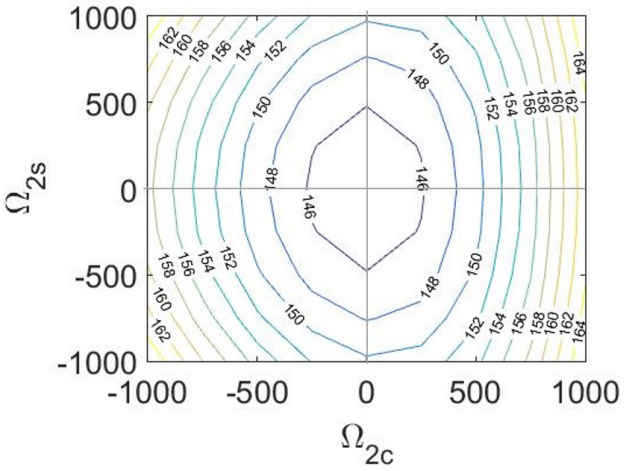

(a) Power (W), Hover

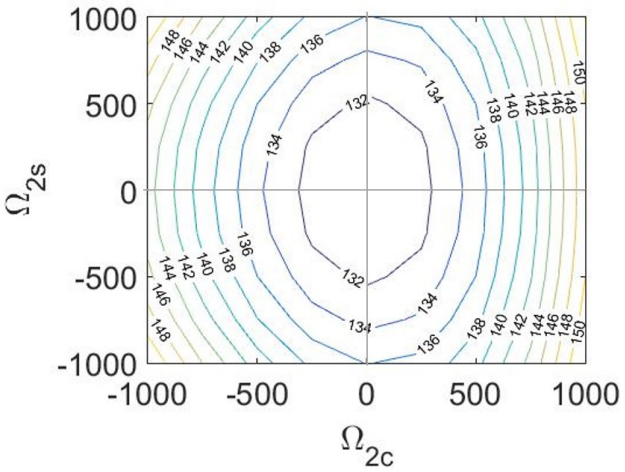

(b) Power (W), 5 m/s

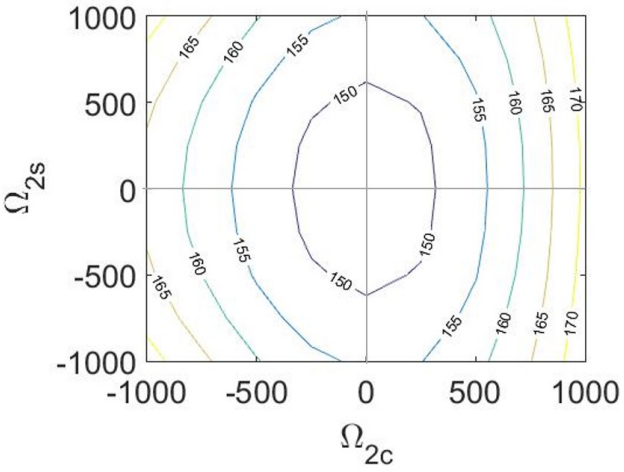

(c) Power (W), 10 m/s

Fig. 16. Power requirements for the hexacopter (Watts)

Octocopter

Trim results over a 0-10 m/s speed range were examined for an octocopter in the edge-first orientation. The trim solution with zero redundant controls is presented in Fig. 17.

Similar to the hexacopter, the octocopter helicopter requires only collective and pitch control to trim in forward flight. The nose-down pitch attitude increases with increasing forward speed so thrust from the rotors an provide the propulsive force to overcome drag.

Next, Ω_{2s} is parametrically varied, and the required trim controls are plotted in Fig. 18. Ω_{2s} affects collective and roll control in the same way as it does in the hexacopter, and also does not affect the required pitch control. However, yaw control is not significantly affected by Ω_{2s}, remaining approximately zero at all speeds.

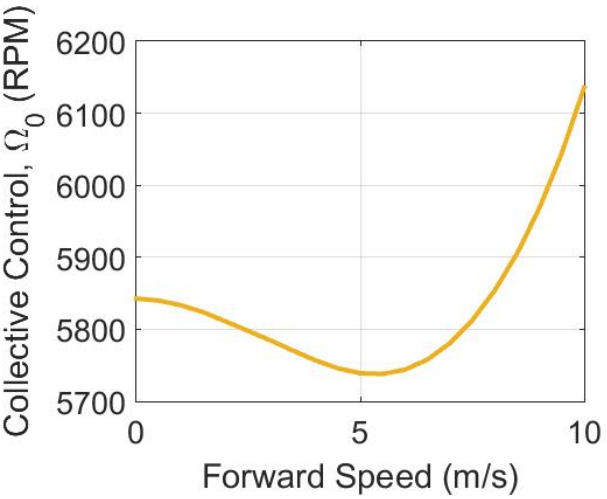

(a) Collective Control

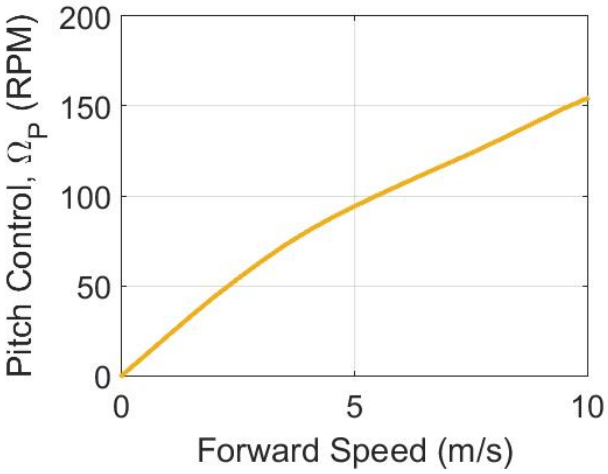

(b) Pitch Control

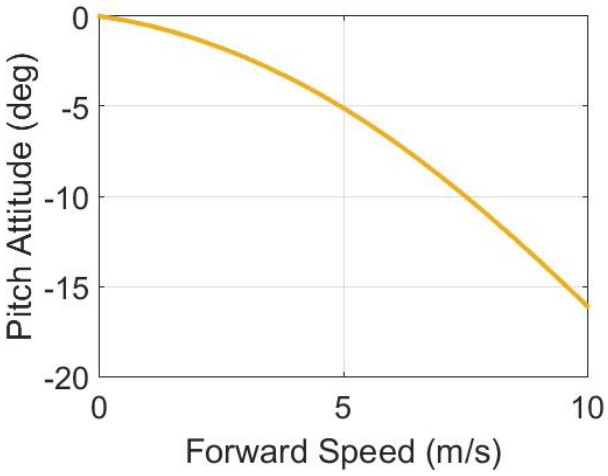

(c) Pitch Attitude

Fig. 17. Trim Controls for octocopter helicopter

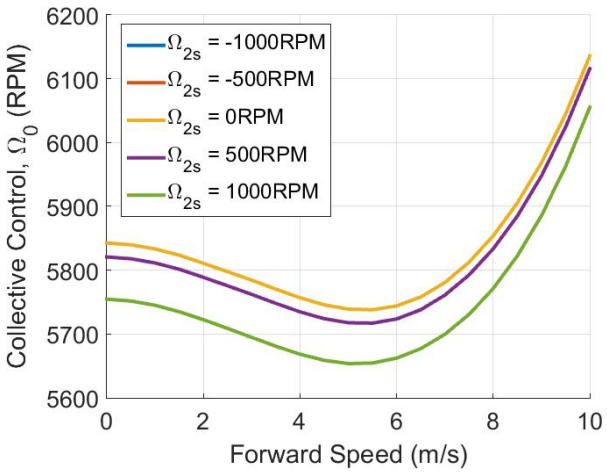

(a) Collective Control

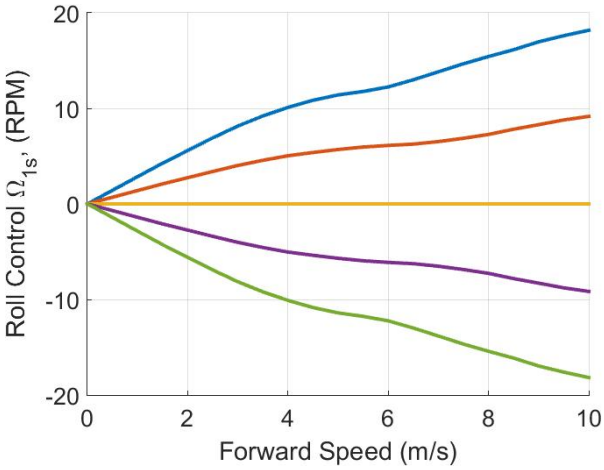

(b) Lateral Control

Fig. 18. Octocopter trim solutions as Ω_{2s} is varied

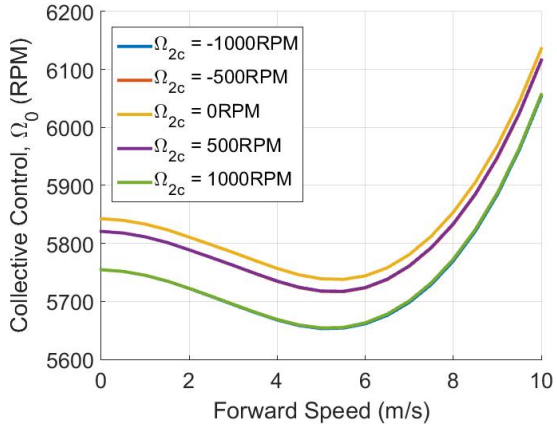

(a) Collective Control

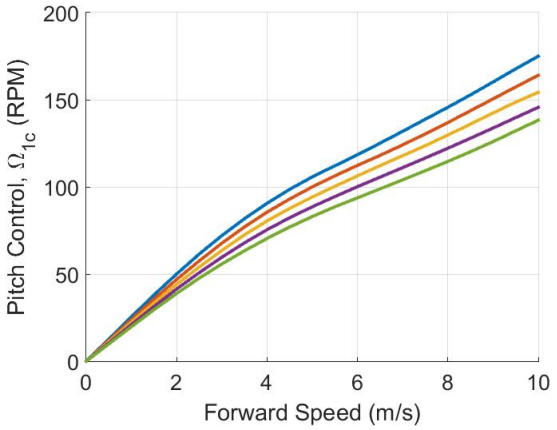

(b) Pitch Control

Fig. 19. Octocopter trim solutions as Ω_{2c} is varied

Trim controls as Ω_{2c} is varied are presented in Fig. 19. Again, collective control is reduced when any Ω_{2c} is applied. Lateral and yaw control are completely unafffected, remaining identically zero. Pitch control is reduced for increasing Ω_{2c}. This is because positive Ω_{2c} shifts lift from the lateral rotors to the longitudinal ones, increasing the effectiveness of pitch control, thus reducing the required Ω_{1c}.

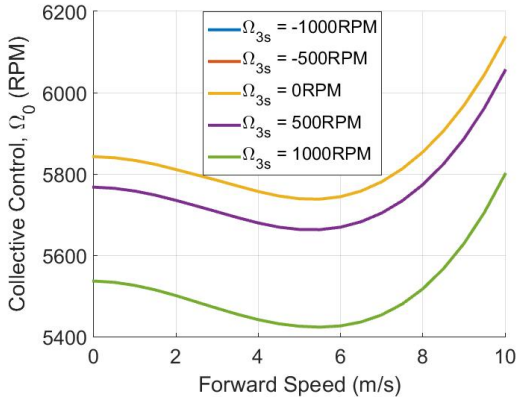

(a) Collective Control

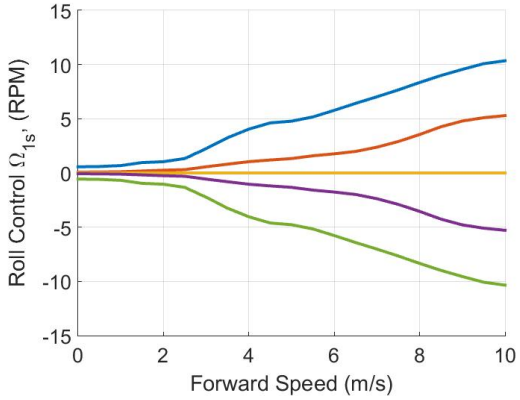

(b) Lateral Control

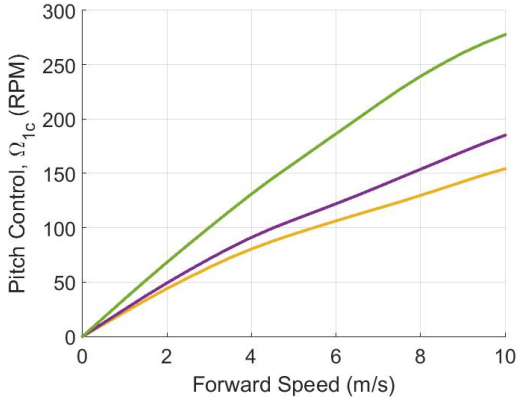

(c) Pitch Control

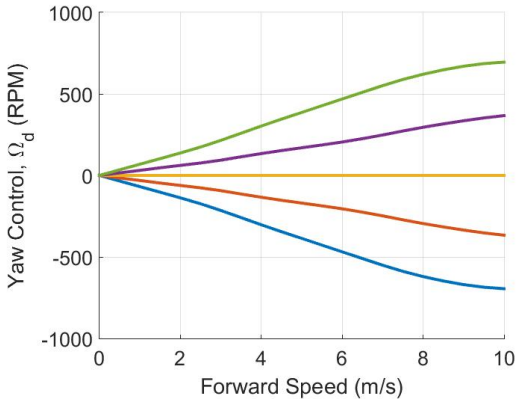

(d) Yaw Control

Fig. 20. Octocopter trim solutions as Ω_{3s} is varied

Next, the effect of Ω_{3s} (roll share mode) is examined. Of all the redundant modes, the roll-share mode has the largest effect on the primary controls, mist significantly on the collective and yaw controls, followed by the pitch control, and finally a small effect on the roll control.

Finally, Ω_{3c} is varied, and the trim solutions plotted in Fig. 21. The pitch-share mode, again, results in a reduction in the collective control requirement, but does not effect any of the other primary controls.

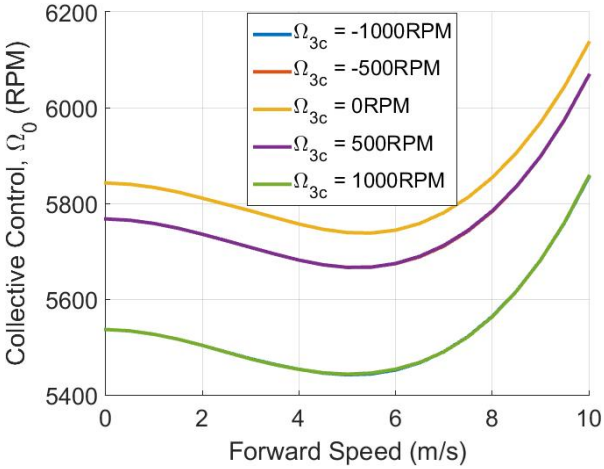

Fig. 21. Collective Control variation with Ω_{3c}

Figure 22 shows power requirements at hover, and at 5 m/s and 10 m/s forward speed, with the addition of the redundant controls. At all of these flight conditions, it is oberved that the minimum power corresponds to zero redundant controls. The power penalty associated with the use of the roll and pitch-share modes (Ω_{3c} and Ω_{3c}) is greater than that with the use of the twist modes ($\Omega 2s$ and Ω_{2c}.

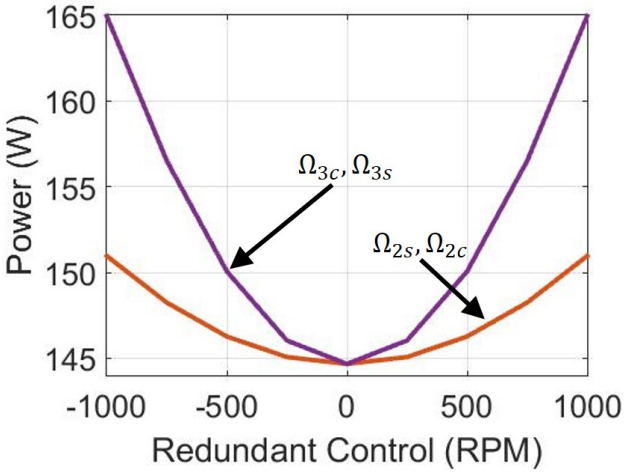

(a) Hover

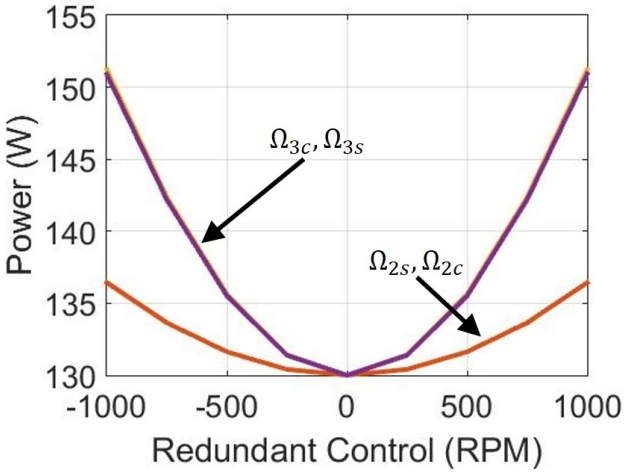

(b) $V_\infty = 5$ m/s

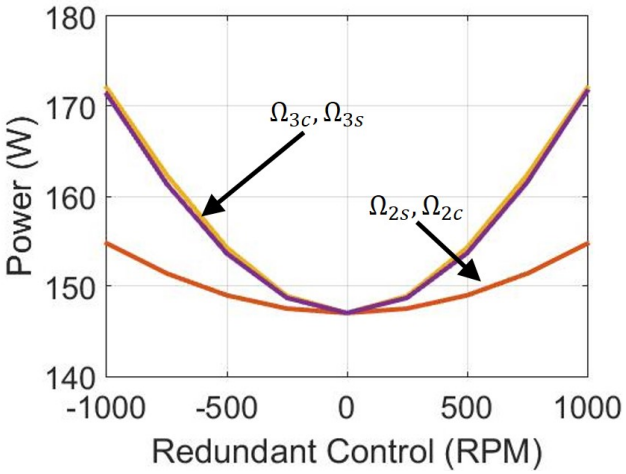

(c) $V_\infty = 10$ m/s

Fig. 22. Power Requirements for Octocopter helicopter

FLIGHT DYNAMICS

Dynamic Modes of the Hexacopter

The poles of the hexacopter (in the vertex-first orientation) in hover condition are plotted in Fig. 23, all of which are in the left half-plane, indicating that the hexacopter is stable in hover. There are four poles located at the origin, corresponding to the three positional states, which do not contribute to the accelerations (ground effect and atmospheric changes not modeled), and the heading, which in hover also has zero effect on the dynamics of the aircraft. Additionally, four more poles lie on the real axis, at three distinct values. The rightmost pole is the yaw mode, where the aircraft spins about its yaw axis, with aerodynamic drag damping the motion. In the middle is the heave mode, damped by changes in the rotor downwash caused by heave. On the left are two modes: pitch and roll subsidence, which coincide because the aircraft is radially symmetric.

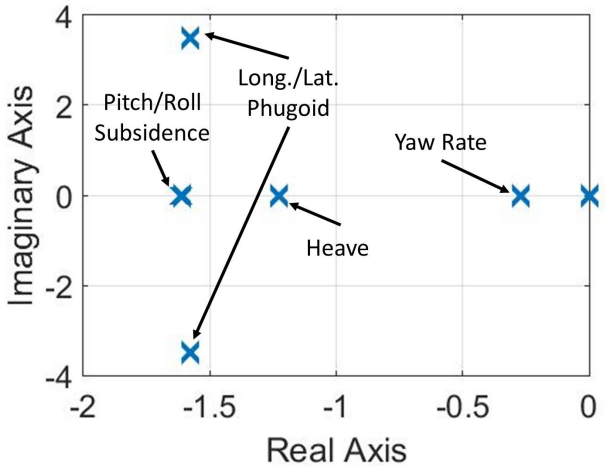

Fig. 23. Poles of the hexacopter helicopter in hover

Finally, there are two pairs of complex conjugate poles corresponding to a longitudinal and lateral phugoid mode. These two modes, like the subsidence modes, are coincident due to the aircraft's symmetry. The longitudinal phugoid mode begins with a nose-down pitch attitude, which causes the aircraft to begin traveling forward. The forward travel induces a nose-up pitching moment on the rotors, due to longitudinal inflow distribution (Ref. 7), causing the aircraft to begin pitching nose-up. Damping on this mode is provided by pitch rate, which, in the case of nose-up pitch rate, causes rotors in the front of the aircraft to climb, increasing their downwash and reducing their thrust. The opposite happens on the aft of the aircraft, providing a damping moment in the pitch direction. The longitudinal phugoid mode is illustrated in Fig. 24, beginning with a nose down attitude (Fig. 24, 1), traveling forward (Fig. 24, 2-4), reaching a maximum (Fig. 24, 5), and returning to the start (Fig. 24, 6-8). It should be noted that although the return trip is depicted below the advancing trip,

this mode has no vertical displacement in hover. The lateral phugoid mode is identical to the longitudinal phugoid mode, with roll substituted for pitch and lateral travel for forward travel.

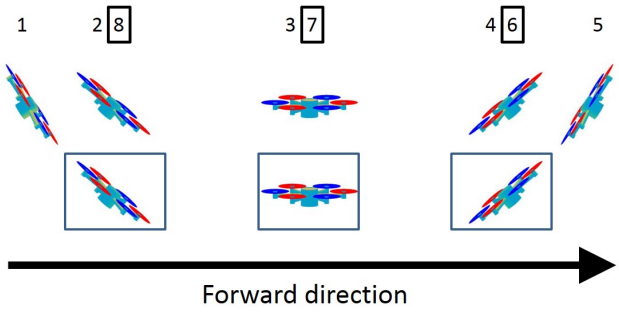

Fig. 24. Longitudinal Phugoid mode in hexacopter helicopter – Return trip offset for clarity

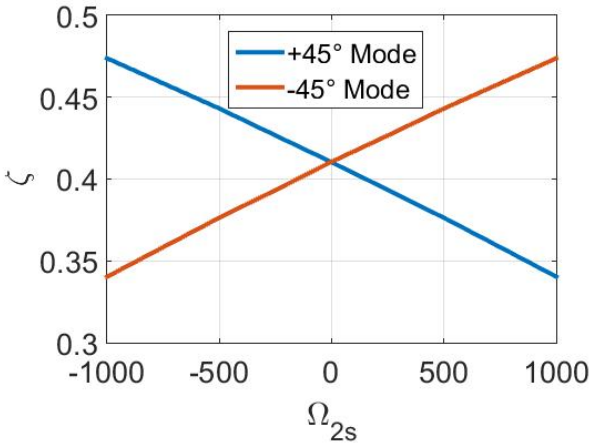

(a) Ω_{2s}

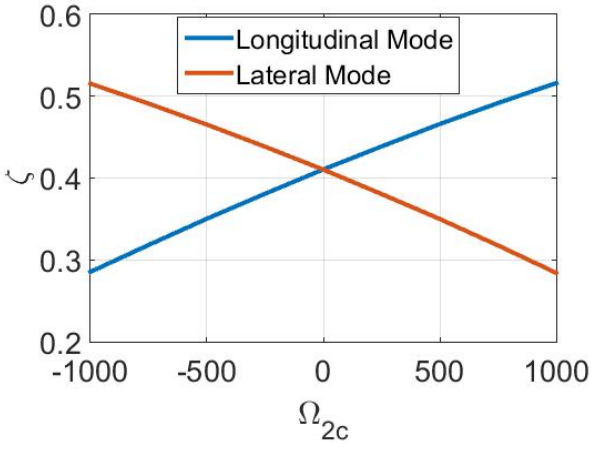

(b) Ω_{2c}

Fig. 25. Variation of hexacopter phugoid mode damping ratios with second harmonic controls

When either of the redundant controls are varied, the symmetry of the aircraft is lost, and the two phugoid modes become distinct. As Ω_{2s} is applied, lift is shifted from rotors 3 and 6 (numbering in Fig. 2(a)) onto rotors 2 and 5. This enhances the damping in the 2-5 direction, at the expense of damping in the 3-6 direction. This causes the phugoid modes to oscillate along axes offset $\pm 45°$ from the longitudinal axis. The damping ratios of the two modes are plotted in Fig. 25(a), where the $+45°$ mode goes forward and to the right, and the $-45°$ goes forward and to the left.

When Ω_{2c} is changed from zero, lift is shifted from rotors 2, 3, 5, and 6 (See Fig. 2(a)) onto rotors 1 and 4. This will enhance damping in the 1-6 direction, while reducing damping normal to the 1-6 direction. Therefore, positive Ω_{2c} will increase the stability of the longitudinal phugoid mode, while reducing that of the lateral phugoid mode. Unlike Ω_{2s}, the directionality of the phugoid modes is unchanged. The damping ratios are plotted in Fig. 25(b).

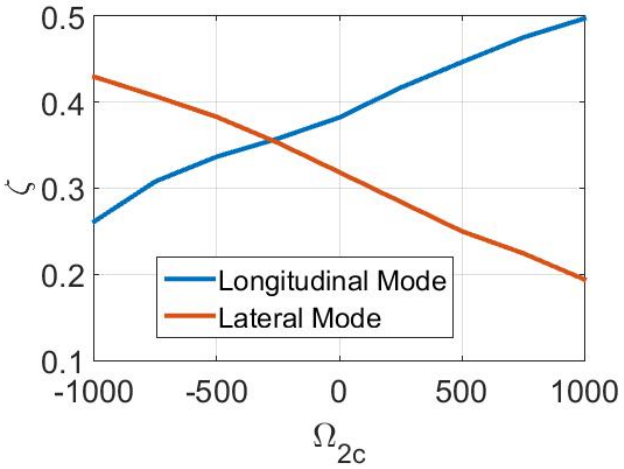

Fig. 26. Change of the phugoid mode damping ratios with Ω_{2c} at 5m/s

In hover, there is no real benefit to using either of the redundant controls in terms of the stability of the longitudinal and lateral phugoid modes. However, in forward flight, the longitudinal phugoid mode becomes more stable than the lateral phugoid mode. Through use of negative Ω_{2c}, some of the stability of the longitudinal phugoid mode can be transferred to the lateral mode, as in Fig. 26. Relative to the power-optimal solution, the stability of the lateral phugoid mode increases 10% through use of this redundant control, at less than 1% cost in power (Fig. 16(b)).

Dynamic Modes of the Octocopter

The same approach to dynamic mode analysis is applied to the octocopter in the edge-first orientation. The nonlinear model is linearized about a trim point, and then static condensation is applied to obtain an equation in the form of 15. The control

vector is set to zero, and then the eigenvalues and eigenvectors of $\bar{A}$ are calculated. The poles of the system about the hover condition are plotted in figure 27.

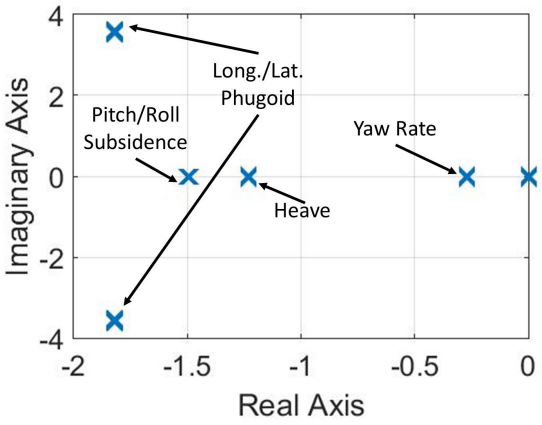

Fig. 27. Rigid body poles of the octocopter helicopter in hover

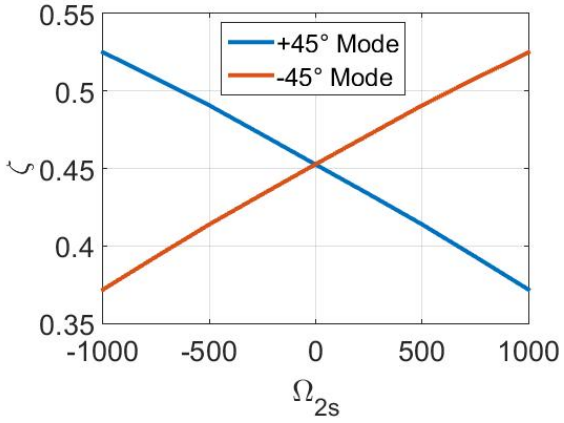

(a) Ω_{2s}

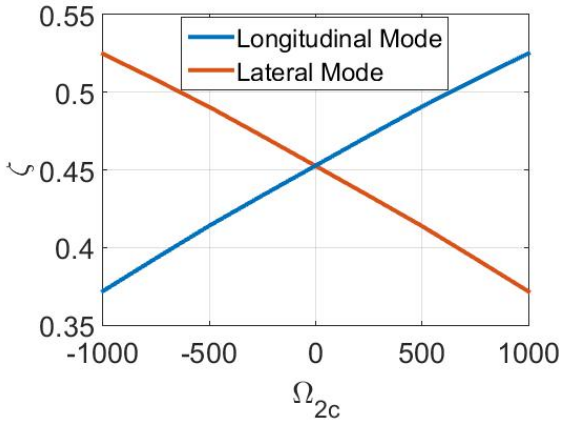

(b) Ω_{2c}

Fig. 28. Variation of octocopter phugoid mode damping ratios with second harmonic controls

As with the hexacopter, four poles are at the origin, corresponding to the position and heading. There are four more poles on the real axis, corresponding to, from right to left, the yaw mode, heave mode, and the pitch/roll subsidence modes (coincident). Finally, there are two pairs of complex conjugate poles, corresponding to the longitudinal and lateral phugoid modes, which are qualitatively similar to those of the hexacopter. As with the hexacopter, the symmetry of the aircraft causes the subsidence and phugoid modes to be coincident in hover, when no redundant controls are applied.

When Ω_{2s} is applied, lift is shifted from the $\Psi = 135°$-$-315°$ line onto the $\Psi = 45° - 225°$ line. This causes the phugoid modes to become aligned with these axes, as well as affecting their stability (Fig. 28(a)).

As positive Ω_{2c} is applied, lift is shifted from the $\Psi = 90°$-$-270°$ line onto the $\Psi = 0° - 180°$ line, which causes the longitudinal phugoid mode to become more stable at the expense of the stability of the lateral mode while the direction of oscillation is unchanged (Fig. 28(b)). As in the case of the hexacopter, this redundant control can be used in forward flight to increase the stability of the lateral phugoid mode, which is less stable in forward flight, at the expense of the longitudinal phugoid mode, which is more stable at the power-optimal solution.

Application of positive or negative Ω_{3s} (Fig. 29(a)) or Ω_{3c} (Fig. 29(b)) serves to slightly reduce the damping ratio of both phugoid modes. Neither control changes the direction of the phugoid modes.

Similar to the hexacopter, use of the redundant control modes does not improve overall stability in hover, since additional stability of one mode comes at the expense of another mode. However, in forward flight, Ω_{2c} can be used to improve the stability of the lateral phugoid mode, which is less stable in forward flight than the longitudinal phugoid mode.

CONCLUSIONS

This study develops the multi-rotor coordinate transformation, and for hexacopters and octocopters identifies primary and redundant controls in multi-rotor coordinates. For hexacopters, the control modes in multi-rotor coordinates comprise of four primary control modes (the collective, roll, pitch and yaw modes), and two redundant modes (twist and lift-share modes). Based on a comparison of the vertex-first and edge-first orientations the collective and yaw control modes were found to be the same. For the vertex-first case, all six rotors are used for pitch control and for the edge-first case all six rotors are used for roll control. In these cases, the RPM change associated with the vertex rotors is twice that used for the rotors closes to the lateral and longitudinal axes, respectively. Both the vertex-first and the edge-first orientations have two redundant control modes that can be characterized as twist and lift-share modes. The latter redistributes lift between the vertex rotors and the rotors closer to the lateral or longitudinal axes.

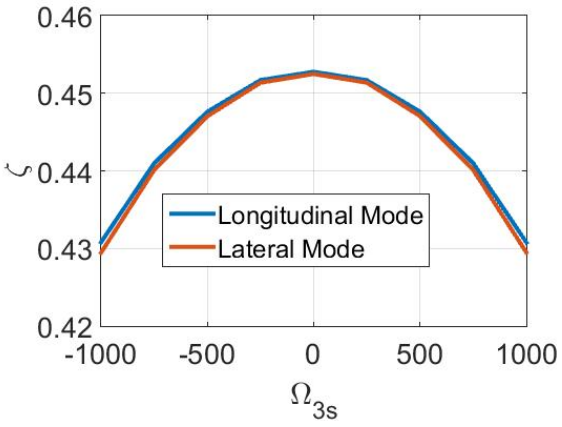

(a) Ω_{3s}

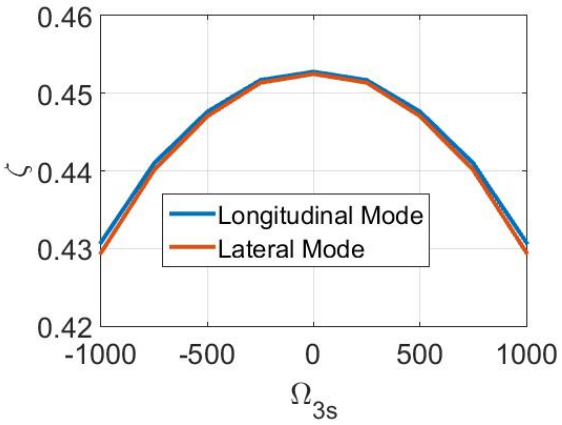

(b) Ω_{3s}

Fig. 29. Variation of octorotor phugoid mode damping with third harmonics controls

For octocopters, in multi-rotor coordinates, in addition to the four primary control modes (collective, roll, pitch and yaw modes), there are four redundant modes. The collective and yaw control modes are similar for the vertex-first and edge-first orientations. The roll and pitch control modes use all 8 rotors for the edge-first case, but only 6 rotors for the vertex-first case since the latter has two rotors on the longitudinal axis (that provide no roll authority) and two on the lateral axis (that provide no pitch authority). The Ω_{2s}, Ω_{2c} redundant modes apply a twisting action to both the vertex-first and edge-first orientations. For the vertex-first orientation, the Ω_{2s} mode can also be identified as lift-share mode between clockwise spinning rotors, and the Ω_{2c} mode can similarly be identified as a lift-share mode between the counterclockwise rotors. For both octocopter orientations, the Ω_{3s} and Ω_{3c} redundant modes are roll-share and pitch-share modes, respectively, but as with the primary roll and pitch control modes, the vertex-first orientation uses only 6 rotors as opposed to the edge-first orientation which uses all 8.

For the hexacopter in the vertex-first orientation, the use of the redundant controls on the trim was examined over a 0-10 m/s speed range. The Ω_{2s} twist mode resulted in small changes in the collective, roll and yaw control, with a Ω_{2s} of 1000 RPM resulting in changes of less than 50RPM in the primary controls. The lift-share mode, on the other hand, resulted in larger changes in the collective, pitch and yaw controls (Ω_{2c} of 1000 RPM showed changes of around 200 RPM in collective and pitch controls, and changes of up to 600 RPM in yaw control). Its effect on roll control input was smaller (under 20 RPM). The twist and lift-share redundant modes increased the power requirement at all flight speeds, demonstrating that the minimum power flight is achieved through the use of only the primary controls (and zero redundant controls).

For the octocopter in the edge-first orientation, the use of the redundant controls on the trim was examined over a 0-10 m/s speed range. The roll-share mode requires the largest changes in the primary controls, most significantly in the collective and yaw controls, followed by the pitch control, and only a small change in the roll control. The pitch-share mode reduces the collective control requirements only, and does not affect any of the other primary controls. Both the twist modes result in reductions in collective control, with the Ω_{2s} also requiring a smaller change in roll control, and the Ω_{2c} similarly requiring a smaller change in pitch control. As with the hexacopter, the redundant modes increased the power requirement at all flight speeds, demonstrating once again that the minimum power flight is achieved through the use of only the primary controls (and zero redundant controls).

The eigenvalues and eigenvectors from the linearized models were used to examine the flight dynamics of the hexacopter and octocopter from hover up to 10 m/s. For both the hexacopter and octocopter, the only oscillatory modes in hover were the longitudinal and lateral phugoid modes. The former coupled longitudinal translation and pitch, while the latter coupled lateral translation and roll, and without the use of any redundant controls the poles of the two phugoid modes were coincident. For both the hexacopter and the octocopter, the Ω_{2s} and Ω_{2c} redundant modes influence the phugoid mode damping, but since they destabilize one mode while stabilizing the other, there appears to be no net benefit to using them. In forward flight, the longitudinal phugoid mode picks up altitude change and becomes more stable than the lateral phugoid mode. For a hexacopter (vertex-first orientation) it was observed that the damping of the lateral phugoid mode could be improved by 10% (at a 1% power penalty), by using the lift-share (Ω_{2c}) redundant mode.

REFERENCES

[1]Kaufman, E., Caldwell, K., Lee, D., Lee, T., "Design and Development of a Free-Floating Hexrotor UAV for 6-DOF Maneuvers" 2014 IEEE Aerospace Conference, Big Sky, Montana, March 1-8, 2014.

[2]Haines, J., Cover H., and Chambers, A., "Modeling and Control of an Octorotor", The Robitics Institute, Carnegie Mellon University, Pittsburgh, Pennsylvania.

[3]Merheb, A., Bateman, F., and Noura, H., "Passive and Active Fault Tolerant Control of an Octorotor UAV Using Sec-

ond Order Sliding Mode Control" 2015 IEEE Conference on Control Applications, 2015 IEEE Multi-Conference on Systems and Control, September 21-23, 2015, Sydney Australia.

[4]Bergman, K., and Ekström., "Modeling, Estimation and Attitude Control of an Octorotor Using PID and $\mathscr{L}_1$ Adaptive Control Techniques", Master's thesis, Linköping University, Linköping, Sweden.

[5]Nakamura, T., Haviland., S., Bershadsky, D., and Johnson., E., "Vision-Based Optimal Landing on a Moving Platform" 72nd Annual Forum of the American Helicopter Society International, May 17-19, 2016, West Palm Beach, Florida.

[6]Russel, C., Jung, J., Willink, G., and Glasner, B., "Wind Tunnel and Hover Performance Test Results for Multicopter UAS Vehicles" 72nd Annual Forum of the American Helicopter Society International, May 17-19, 2016, West Palm Beach, Florida.

[7]Niemiec, R., and Gandhi, F., "Effect of Inflow Model on Simulated Aeromechanics of Quadrotor Helicopters" 72nd Annual Forum of the American Helicopter Society International, May 17-19, 2016, West Palm Beach, Florida.

[8]Niemiec, R., and Gandhi, F., "Differences Between Quadrotor Helicopter Flight Configurations", 42nd European Rotorcraft Forum, September 5-8, 2016, Lille, France.

[9]Johnson, W., "Helicopter Aeromechanics", Cambridge University Press, New York, NY, 2013, pp. 549-562.